Interplay of Electron and Nuclear Spin Noise in *n*-Type GaAs

Fabian Berski,[1] Jens Hübner,[1,*] Michael Oestreich,[1,†] Arne Ludwig,[2] A. D. Wieck,[2] and Mikhail Glazov[3,4,‡]

[1]*Institut für Festkörperphysik, Leibniz Universität Hannover, Appelstraße 2, D-30167 Hannover, Germany*
[2]*Angewandte Festkörperphysik, Ruhr-Universität Bochum, 44780 Bochum, Germany*
[3]*Ioffe Institute, Polytechnicheskaya 26, 194021 St. Petersburg, Russia*
[4]*Spin Optics Laboratory, St. Petersburg State University, Ul'anovskaya 1, Peterhof, 198504 St. Petersburg, Russia*

We present spin-noise spectroscopy measurements on an ensemble of donor-bound electrons in ultrapure GaAs:Si covering temporal dynamics over 6 orders of magnitude from milliseconds to nanoseconds. The spin-noise spectra detected at the donor-bound exciton transition show the multifaceted dynamical regime of the ubiquitous mutual electron and nuclear spin interaction typical for III-V-based semiconductor systems. The experiment distinctly reveals the finite Overhauser shift of an electron spin precession at zero external magnetic field and a second contribution around zero frequency stemming from the electron spin components parallel to the nuclear spin fluctuations. Moreover, at very low frequencies, features related with time-dependent nuclear spin fluctuations are clearly resolved making it possible to study the intricate nuclear spin dynamics at zero and low magnetic fields. The findings are in agreement with the developed model of electron and nuclear spin noise.

Harnessing coherence is one of the central topics in current research and attracts high interest due to the complex fundamental physics bridging quantum mechanics and statistics as well as due to prospective applications for information processing [1–3]. The solid state quantum states based upon the spin degree of freedom of confined carriers in semiconductors are at the forefront of many current research activities in this field. In this respect, optically addressable electron and hole spin quantum states in III-V-based semiconductor systems bear the beauty of efficient options for initialization, manipulation, and read-out by light in combination with exceptional sample quality [4]. Currently, a promising system for these tasks are donor-bound electrons in ultrahigh quality, very weakly *n*-doped GaAs since the widely spaced, quasi-isolated electrons act as an ensemble of identical, individually localized atoms [5,6]. However, the ostensible catch of this approach is the inherent interaction with the nuclear spin bath which has been addressed in many different systems so far [7–11].

In principle, there are different approaches to deal with the decoherence imposed via the hyperfine interaction. On the first sight, the most obvious way is to replace the isotopes carrying a nuclear spin with spinless isotopes like in ^{28}Si [12] but silicon has the drawback of an indirect gap. Direct semiconductors with spinless isotopes like, e.g., isotopically purified II-VI systems have yet the drawback of inferior sample quality. In single III-V-based quantum dots, the hyperfine interaction can be reduced by either moving on to hole spins which show a diminished hyperfine interaction [13–15] or by polarizing the nuclei in order to make them less effective [16,17]. Besides that, the mutual interaction between carrier and nuclear spins is

also strain dependent and strongly varying coupling strengths in such nanostructures result in a row of widely discussed problems with the central spin problem being one of the most prominent and complex examples [9,18]. By contrast, donor-bound electrons in high purity bulk GaAs have an isotropic, well-defined hyperfine interaction in a strain-free environment, in which case an in-depth understanding and exploitation of the generic electron and nuclear spin dynamics looks feasible.

Measurements of the intrinsic spin dynamics of weakly interacting donor-bound electrons in GaAs are extremely challenging since any optical excitation of free carriers dramatically affects their spin dynamics. The Hanle effect [19] and the resonant spin amplification technique [20] both involve considerable optical excitation, which alters the spin dynamics and results in a complex picture involving the spin relaxation of resident and photocreated charge carriers. In this Letter, we avoid this problem by utilizing spin-noise (SN) spectroscopy and demonstrate in the limit of low excitation densities the intrinsic spin dynamic of the donor-bound electron ensemble. This nearly perturbation-free quantum optical method [21–25] allows us to observe the intricate interplay of the electron and nuclear spin dynamics with high resolution on unmatched time scales ranging from nanoseconds to milliseconds. Furthermore, the direct observation of the nuclear spin Faraday effect at thermal equilibrium leads to manifestations of nuclear spin fluctuations in the linear optical response. This paves the way for using SN spectroscopy as an efficient, alternative experimental tool to optically detected magnetic resonance.

Figure 1(a) depicts the studied physical situation. The sample consists of a $d = 10 \ \mu$m thick, very high purity
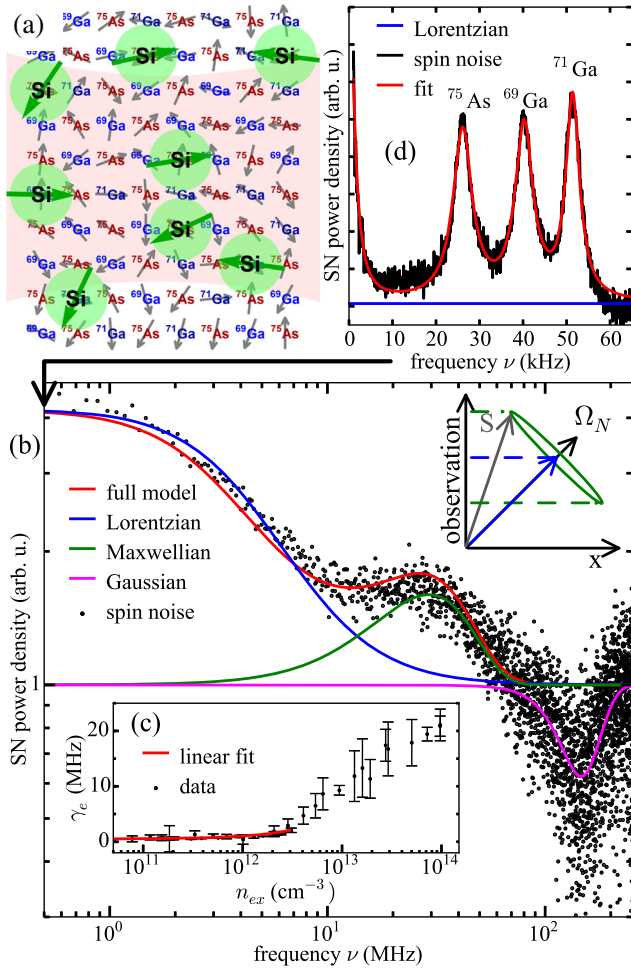
FIG. 1 (color online).   (a) Experimental situation (not to scale): laser light (red) samples the spin dynamic of an ensemble of Si-donor-bound electrons (green) each interacting with $\sim 10^5$ nuclear magnetic moments. (b) Black dots are the SN difference spectrum of donor-bound electrons (at $B = 0$ mT minus at $B = 22$ mT) measured at $P = 1$ μW. The red line is a fit according to the model of Ref. [26]; blue, green, and magenta curves represent the individual contributions (see text). The spectrum is rescaled and shifted to positive noise power densities. (c) Measured width of the homogeneous SN contribution [blue curve in (a)] as a function of the photogenerated exciton density n_{ex}. The red line is a linear fit extrapolating to $\gamma_0 = 0.50 \pm 0.09$ MHz. (d) SN difference spectrum (black line) in the low-frequency range measured at $P = 1$ μW and $B = 3.75$ mT. Contributions from the individual host lattice isotopes are clearly resolved and labeled respectively. See text for details on the nuclear $\nu = 0$ feature. All measurements were performed at $T = 4.2$ K and a quasiresonant probe.

GaAs layer grown by molecular beam epitaxy on top of a semi-insulating GaAs substrate separated by a GaAs/AlAs superlattice and an AlAs etch stop buffer layer. The intentional n-type doping density of the GaAs:Si layer is $n_D \approx 1 \times 10^{14}$ cm^{-3} which yields an average distance between two neighboring Si donors of about 20 Bohr radii. The hydrogenlike wave function of each localized

electron overlaps with $\sim 10^5$ host lattice nuclear magnetic moments leading to contact hyperfine interaction [27]. A via hole with a diameter of approximately 100 μm is wet chemical etched through the backside of the sample [28] to gain unobstructed optical access to the molecular-beam-epitaxy-grown GaAs for transmission measurements.

The sample is mounted in a cold finger cryostat and cooled down to temperatures between 3.8 and 11 K. An electromagnet is used to apply transverse magnetic fields B up to 40 mT with respect to the direction of light propagation. Linearly polarized laser light is focused to a beam waist of 4.5 μm and tuned quasiresonantly to the maximum of the inhomogeneously broadened donor-bound exciton ($D^0 X$) transition at $E_0 = 1514.26$ meV with a full width at half-maximum of $\Delta_{\text{FWHM}} \approx 150$ μeV measured by absorption spectroscopy. The spin induced stochastic Faraday rotation (spin noise) of the transmitted laser light is resolved by a polarization bridge and a low-noise balanced photo receiver [30]. The noise background due to optical and electronic noise is eliminated by subtracting SN spectra with a different transverse magnetic field from each other [45].

Figure 1 shows measured SN spectra in the frequency range from 1 kHz to 250 MHz. We start the discussion with the SN power density between 0.5 and 250 MHz which is shown in Fig. 1(b) as the difference [46] of SN acquired at $B = 0$ mT and at $B = 22$ mT (black dots). Here, the two contributions with power density > 1 centered at $\nu = 0$ and $\nu = \nu_o \approx 30$ MHz stem from the measurement at zero external field while the data with density < 1 are measured at finite B. This classification is justified because the external applied magnetic field is strong enough to shift the SN signal away from zero frequency as discussed below. The peak at ν_o arises from electron spin precession in the quasistatic field of nuclear fluctuations, i.e., from the precession in the randomly distributed Overhauser fields Ω_N [7] [see pictogram in Fig. 1(b)]: their random distribution at different donor sites results in a Maxwell-like SN shape [26,47] $S_M(\nu) = 8 A_M \pi^{-1/2} \delta_e^{-3} \nu^2 \exp(-\nu^2/\delta_e^2)$ [Fig. 1(b), green line]. Here, A_M is the respective noise power, and δ_e results from the dispersion of the nuclear fields Δ_B as $\delta_e = g_e \mu_B \Delta_B/(2\pi\hbar) = 1/(2\pi T_\Delta)$, where g_e is the electron g factor. The feature at $\nu = 0$ in Fig. 1(b) arises from the electron spin component parallel to Ω_N, which is conserved in the course of fast electron spin precession [pictogram in Fig. 1(b)] [7,47]. This contribution is approximated by a Lorentzian shape [blue line in Fig. 1(b)], i.e., $S_L(\nu) = A_L 2\gamma_e/[\pi(\nu^2 + \gamma_e^2)]$ with $2\pi\gamma_e$ being the damping related to a finite electron correlation at a given donor [26] and to spin-flip processes not related to hyperfine interaction [47]. Such a specific two-peak structure is a distinct feature of the SN of localized electrons coupled to lattice moments and, moreover, the simultaneous presence of both contributions in the zero field spectrum clearly demonstrates that the correlation

time of hyperfine fluctuations experienced by an electron τ_c is long, i.e., $\tau_c > T_\Delta$ [26].

The SN feature at $\nu \approx 140$ MHz results from the Larmor precession of the stochastically oriented electron spin ensemble in the effective magnetic field given by the sum of the local hyperfine fields and the applied transverse magnetic field. In agreement with Refs. [26,47] this feature is well described by a Gaussian function $S_G(\nu) = (A_G/\sqrt{2\pi\delta_e^{*2}}) \exp\left[-\frac{1}{2}(\nu - \nu_L)^2/\delta_e^{*2}\right]$ shown as magenta line in Fig. 1(b). Here, A_G is the SN power of the precession contribution, $\nu_L = g_e\mu_B B/2\pi\hbar$ is the Larmor frequency, and δ_e^* is the spread of the spin precession frequencies caused by nuclear fields and g-factor variations [47]. By fitting $S_G(\nu)$ to the data, an electron g factor of $|g_e^*| = 0.46 \pm 0.064$ [48] is extracted in concurrence with the literature [49].

All extracted fit parameters are summarized in Table I. The width of the precession peak at ν_L is increased by about 15% compared to the Overhauser contribution which is attributed to an electric field dependent g-factor spread [30,50]. Furthermore, the consistency of the fit is demonstrated by the general conservation of SN power: $A_G = A_L + A_M$ which describes the lossless redistribution from the Larmor precession peak at $B \neq 0$ towards the two-peak structure at $B = 0$. Interestingly, the power ratio of the homogeneous and the Overhauser contribution $A_L/A_M \approx 2$ deviates strongly from the expected $1/2$ ratio [26,47] and is caused by a finite value of the electron correlation time at a given donor: overall, the two $B = 0$ features are very well modeled with Eqs. (6) and (9) of Ref. [26] including (i) spin precession in the random hyperfine fields and (ii) the finite correlation time τ_c. The model [red curve in Fig. 1(b)] is fitted to the data with τ_c and δ_e being the only free parameters and allows us to extract the nuclear field spread, $\delta_e \approx 29 \pm 0.3$ MHz. This corresponds to $\Delta_B \approx 4.6$ mT, which is in close agreement with other experimental data [19,51] as well as with the value extracted from the Maxwellian fit. The correlation time of $\tau_c \approx 32 \pm 0.6$ ns is very close to the value reported in Ref. [19] for a comparable electron density. The Lorentzian fit of the zero-frequency peak gives a similar value of $\tau_c = (2\pi\gamma_e)^{-1} \approx 37$ ns.

In order to identify the origin of the correlation time τ_c, the dependence of the zero-frequency component of the electron SN on the photogenerated excitation density n_{ex} is

measured by reducing the bandwidth of the used detector which is accompanied with increased optical sensitivity [52]. This allows us to accumulate SN at very low optical powers and eliminates the creation of free carriers due to residual photon absorption. The measured spectra are fitted by the Lorentzian function $S_L(\nu)$ and the resulting dependence $\gamma_e(n_{\text{ex}})$ is depicted in Fig. 1(c) over more than 3 orders of magnitude. The strong sensitivity of γ_e and, hence, of τ_c on the probe power demonstrates that the correlation time can be controlled by optical excitation, i.e., by photo-creation or photoassisted delocalization of electrons. For vanishing n_{ex} we obtain a value of $2\pi\gamma_e = 3.14 \pm 0.6$ MHz corresponding to a correlation or spin relaxation time of about 320 ns. This time is comparable with the broadening induced by the temporal change of the nuclear spin configurations, which arises from the back action with the donor-electron spin [30].

The measured noise power A_L of the zero-frequency electron SN contribution as a function of the transverse magnetic field B is plotted in Fig. 2 (black dots) showing clearly the expected reduction of the zero-frequency peak. The red line is calculated after Eq. (13) of Ref. [47] with the same parameters as used to fit the SN spectrum in Fig. 1(b) and shows excellent agreement. The inset of Fig. 2 depicts A_L as a function of the cryostat temperature. The experimentally observed SN (black dots) reduces drastically with increasing temperature due to thermal ionization of the donors. The red line is a fit according to Blakemore's equation with the two free parameters being the doping density and a temperature offset between the sensor at the heat exchanger of the cryostat and the laser spot [54]. The
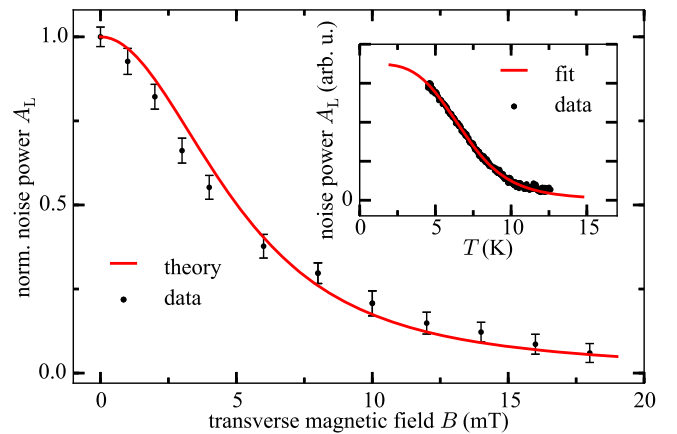

FIG. 2 (color online). Power of the $\nu = 0$ electron spin noise A_L as function of the transverse magnetic field B at $T = 4.2$ K and $P = 270$ nW. The red line is calculated with the model in Ref. [26] with the same parameters as in Fig. 1(b) (note that this theoretical curve is weakly sensitive to the particular value of τ_c). The inset shows the dependence of A_L on the cryostat temperature measured at $B = 0$ mT, $P = 2$ μW, and a detuning $\Delta = -200$ μeV to lower energy. The red line is a fit based on Blakemore's equation [54].

TABLE I. Fit parameters extracted from Fig. 1.

Type	Relative noise power (arbitrary units)	Rate (MHz)
Lorentzian	$A_L = 2.16 \pm 0.03$	$2\pi\gamma_e = 27.1 \pm 1.8$[a]
Maxwell	$A_M = 1.04 \pm 0.02$	$2\pi\delta_e = 182.8 \pm 4.7$
Gaussian	$A_G = 3.22 \pm 0.08$	$2\pi\delta_e^* = 213.6 \pm 11.3$

[a]Reduces to $2\pi\gamma_e = 3.14 \pm 0.6$ MHz for negligible excitation density.

extracted offset is with $\Delta T = 2$ K typical for our cryostat configuration. However, the extracted doping density of 1.5×10^{12} cm^{-3} is much lower than the nominal doping density. The origin of this discrepancy is not fully understood but could be related with unintentional p-type codoping (compensation) and donor depletion due to surface charges.

Now we focus on the very low frequency range, 1 to 70 kHz, which is shown in Fig. 1(d). At a transverse field of $B = 3.75$ mT, the SN spectrum reveals a clearly resolved fine structure consisting of three additional, very narrow SN peaks at finite frequencies. These peaks shift linearly for $B \gtrsim 1$ mT (see Fig. 3) and their origin is identified by the corresponding magnetic moments as the host lattice isotopes ^{75}As, ^{69}Ga, and ^{71}Ga [30]. Interestingly, the relative magnitudes of the nuclear SN do not scale with the different abundances and coupling strengths of the isotopes [55], the origin of which is unclear so far. By fitting the corresponding contributions by Lorentzians [red line in Fig. 1(c)], we extract a ratio $\xi = 1.2 \times 10^{-3}$ of the nuclear SN power for all host lattice isotopes to the zero-frequency electron SN power contribution A_L [30].

The observation of nuclear SN in the Faraday rotation noise spectrum is, at first glance, very surprising, since lattice nuclear spins do not couple directly with light. However, nuclear spin fluctuations affect via hyperfine interaction the electron spin degrees of freedom and manifest themselves in the optical response [56,57]. Particularly, for bulk semiconductors with donor-bound electrons there are two contributions to nuclei-induced Faraday rotation: (i) the Overhauser field induced splitting of the D^0X transition line, which is temperature independent, and (ii) a state-filling effect caused by the electron
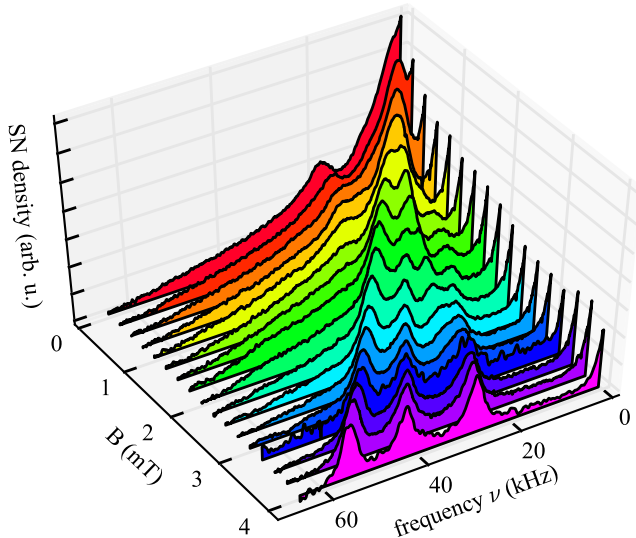
spin polarization in the Overhauser field, which depends on temperature [57]. The straightforward calculation [30] shows that the nuclear fluctuation-induced splitting dominates the SN for quasiresonant detection in an inhomogeneously broadened transition and that the ratio ξ of the nuclei and electron SN powers is given by $\xi \sim (\Delta_N/\Gamma)^2$. Here, $\Delta_N \sim 0.1$–0.3 μeV is the nuclear SN induced energetic fluctuation of the D^0X line and Γ is the *homogeneous* width of the D^0X resonance. Taking $\Gamma = 8$ μeV [58] we estimate $\xi \sim 10^{-4}, \ldots, 10^{-3}$ [30] which is in rather good agreement with the experimentally observed value. This ratio is temperature independent in the studied range between $T = 3.2$ K and $T = 7$ K.

The detection of nuclear spontaneous spin resonance by SN spectroscopy provides the novel method that enables measurements of the nuclear spin dynamics without exciting a nuclear spin polarization [59], applying strong external magnetic fields to split the nuclear spin sublevels, or using radio frequency pulses like in NMR and ODNMR experiments. The suggested technique is particularly useful to address the nuclear spin dynamics at low magnetic fields unaccessible otherwise. Particularly, the measurements at $B \lesssim 1$ mT reveal complex behavior of nuclear spin resonance lines with strong deviations from linear-in-B dependence. These deviations, as well as the appearance of the zero-frequency line in the nuclear SN spectra can be related with small quadrupolar splittings [30], local fields, and intricate nuclear spin decoherence [60] and require further in-depth studies.

In summary, detailed spin-noise measurements on the neutral exciton transition of nearly isolated, localized donor electrons in GaAs yield a comprehensive picture of the intricate electron and nuclear spins at thermal equilibrium including (a) the homogeneous and Overhauser SN contribution at $B = 0$ mT, (b) the influence of the correlation time on their shape and relative noise powers, (c) the temperature dependence of the ionization of a low-density electron ensemble, (d) the inhomogeneous broadening of the Overhauser contribution at finite external magnetic fields due to electron g-factor variations, and (e) the observation of nuclear fluctuations by optical spin-noise spectroscopy and their intricate magnetic field dependence. Especially, the new nuclear-spin-noise technique gives an inimitable access to the nuclear spin dynamics at thermal equilibrium and very low external magnetic fields and promises a variety of applications, i.e., for highly sensitive spatially resolved nuclear magnetic resonance.

FIG. 3 (color online). Nuclear SN spectra as a function of the transverse magnetic field at $T = 4.2$ K and $P = 1$ μW. The homogeneous contribution [blue line in Fig. 1(b)] was subtracted. See text for details.

*jhuebner@nano.uni-hannover.de
†oest@nano.uni-hannover.de
‡glazov@coherent.ioffe.ru

[1] *Semiconductor Spintronics and Quantum Computation*, NanoScience and Technology, edited by D. D. Awschalom, D. Loss, N. Samarth (Springer, Berlin, Heidelberg, 2002).

[2] M. H. Devoret and R. J. Schoelkopf, Science **339**, 1169 (2013).

[3] D. Leibfried, R. Blatt, C. Monroe, and D. Wineland, Rev. Mod. Phys. **75**, 281 (2003).

[4] B. Urbaszek, X. Marie, T. Amand, O. Krebs, P. Voisin, P. Maletinsky, A. Högele, and A. Imamoglu, Rev. Mod. Phys. **85**, 79 (2013).

[5] M. Sladkov, A. U. Chaubal, M. P. Bakker, A. R. Onur, D. Reuter, A. D. Wieck, and C. H. van der Wal, Phys. Rev. B **82**, 121308 (2010).

[6] K.-M. C. Fu, S. M. Clark, C. Santori, C. R. Stanley, M. C. Holland, and Y. Yamamoto, Nat. Phys. **4**, 780 (2008).

[7] I. A. Merkulov, A. L. Efros, and M. Rosen, Phys. Rev. B **65**, 205309 (2002).

[8] A. V. Khaetskii, D. Loss, and L. Glazman, Phys. Rev. Lett. **88**, 186802 (2002).

[9] A. Faribault and D. Schuricht, Phys. Rev. B **88**, 085323 (2013).

[10] P.-F. Braun, X. Marie, L. Lombez, B. Urbaszek, T. Amand, P. Renucci, V. K. Kalevich, K. V. Kavokin, O. Krebs, P. Voisin, and Y. Masumoto, Phys. Rev. Lett. **94**, 116601 (2005).

[11] X. M. Dou, B. Q. Sun, D. S. Jiang, H. Q. Ni, and Z. C. Niu, Phys. Rev. B **84**, 033302 (2011).

[12] G. W. Morley, M. Warner, A. M. Stoneham, P. T. Greenland, J. van Tol, C. W. M. Kay, and G. Aeppli, Nat. Mater. **9**, 725 (2010).

[13] D. Brunner, B. D. Gerardot, P. A. Dalgarno, G. Wüst, K. Karrai, N. G. Stoltz, P. M. Petroff, and R. J. Warburton, Science **325**, 70 (2009).

[14] E. A. Chekhovich, M. M. Glazov, A. B. Krysa, M. Hopkinson, P. Senellart, A. Lemaitre, M. S. Skolnick, and A. I. Tartakovskii, Nat. Phys. **9**, 74 (2013).

[15] R. Dahbashi, J. Hübner, F. Berski, K. Pierz, and M. Oestreich, Phys. Rev. Lett. **112**, 156601 (2014).

[16] G. Sallen, S. Kunz, T. Amand, L. Bouet, T. Kuroda, T. Mano, D. Paget, O. Krebs, X. Marie, K. Sakoda, and B. Urbaszek, Nat. Commun. **5**, 3268 (2014).

[17] D. S. Smirnov, Phys. Rev. B **91**, 205301 (2015).

[18] N. A. Sinitsyn, Y. Li, S. A. Crooker, A. Saxena, and D. L. Smith, Phys. Rev. Lett. **109**, 166605 (2012).

[19] R. I. Dzhioev, K. V. Kavokin, V. L. Korenev, M. V. Lazarev, B. Y. Meltser, M. N. Stepanova, B. P. Zakharchenya, D. Gammon, and D. S. Katzer, Phys. Rev. B **66**, 245204 (2002).

[20] J. M. Kikkawa and D. D. Awschalom, Phys. Rev. Lett. **80**, 4313 (1998).

[21] E. B. Aleksandrov and V. S. Zapasskii, Zh. Eksp. Teor. Fiz. **81**, 132 (1981).

[22] M. Oestreich, M. Römer, R. J. Haug, and D. Hägele, Phys. Rev. Lett. **95**, 216603 (2005).

[23] S. A. Crooker, L. Cheng, and D. L. Smith, Phys. Rev. B **79**, 035208 (2009).

[24] J. Hübner, F. Berski, R. Dahbashi, and M. Oestreich, Phys. Status Solidi (b) **251**, 1824 (2014).

[25] Y. Li, N. Sinitsyn, D. L. Smith, D. Reuter, A. D. Wieck, D. R. Yakovlev, M. Bayer, and S. A. Crooker, Phys. Rev. Lett. **108**, 186603 (2012).

[26] M. M. Glazov, Phys. Rev. B **91**, 195301 (2015).

[27] *The Principles of Nuclear Magnetism*, The International Series of Monographs on Physics, edited by A. Abragam (Oxford University Press, Oxford, 2006).

[28] A mixture of NH_4OH/H_2O_2, followed by citric acid/H_2O_2 and diluted HF to selectively etch the GaAs substrate and the hindering layers is used [29] and results in a surface roughness $< \lambda/10$.

[29] A. R. Clawson, Mater. Sci. Eng. R **31**, 1 (2001).

[30] See Supplemental Material at http://link.aps.org/supplemental/10.1103/PhysRevLett.115.176601, which includes Refs. [31–44], for more details.

[31] G. M. Müller, M. Römer, J. Hübner, and M. Oestreich, Appl. Phys. Lett. **97**, 192109 (2010).

[32] G. H. Fuller, J. Phys. Chem. Ref. Data **5**, 835 (1976).

[33] A. De, C. E. Pryor, and M. E. Flatté, Phys. Rev. Lett. **102**, 017603 (2009).

[34] L. Landau and E. Lifshitz, *Electrodynamics of Continuous Media*, 2nd ed., Course of Theoretical Physics (Butterworth-Heinemann, Oxford, 2004), Vol. 8.

[35] M. M. Glazov, Phys. Solid State **54**, 1 (2012).

[36] V. S. Zapasskii, A. Greilich, S. A. Crooker, Y. Li, G. G. Kozlov, D. R. Yakovlev, D. Reuter, A. D. Wieck, and M. Bayer, Phys. Rev. Lett. **110**, 176601 (2013).

[37] I. A. Merkulov, G. Alvarez, D. R. Yakovlev, and T. C. Schulthess, Phys. Rev. B **81**, 115107 (2010).

[38] K. A. Al-Hassanieh, V. V. Dobrovitski, E. Dagotto, and B. N. Harmon, Phys. Rev. Lett. **97**, 037204 (2006).

[39] W. Yao, R.-B. Liu, and L. J. Sham, Phys. Rev. B **74**, 195301 (2006).

[40] E. Barnes, L. Cywiński, and S. Das Sarma, Phys. Rev. B **84**, 155315 (2011).

[41] *Spin Physics in Semiconductors*, edited by M. Dyakonov (Springer, New York, 2008), pp. 309.

[42] D. S. Smirnov, M. M. Glazov, and E. L. Ivchenko, Phys. Solid State **56**, 254 (2014).

[43] D. Paget, G. Lampel, B. Sapoval, and V. I. Safarov, Phys. Rev. B **15**, 5780 (1977).

[44] *Optical Orientation*, edited by F. Meier and B. Zakharchenya (North-Holland, Amsterdam, 1984).

[45] G. M. Müller, M. Oestreich, M. Römer, and J. Hübner, Physica (Amsterdam) **43E**, 569 (2010).

[46] The difference spectrum is normalized to its minimum and shifted by 1 for the presentation.

[47] M. M. Glazov and E. L. Ivchenko, Phys. Rev. B **86**, 115308 (2012).

[48] The main error results from the uncertainty in the distance between the probe volume and the coils of the electromagnet, i.e., from the uncertainty of the absolute value of the magnetic field at the probe volume.

[49] Kai-Mei C. Fu, C. Santori, C. Stanley, M. C. Holland, and Y. Yamamoto, Phys. Rev. Lett. **95**, 187405 (2005).

[50] The inhomogeneity of B varies in the small probe volume only by 10^{-5}.

[51] J. S. Colton, T. A. Kennedy, A. S. Bracker, J. B. Miller, and D. Gammon, Solid State Commun. **132**, 613 (2004).

[52] The excitation density is calculated via $n_{ex} = P\tau/\hbar\omega \times \{1 - \exp[-\alpha(\hbar\omega)d]\}$ from the laser energy $\hbar\omega$

and the power entering the sample P while a peak absorption of $\alpha(E_0) = 4000$ cm^{-1} and a radiative lifetime of $\tau = 1$ ns [53] is assumed.

[53] E. Finkman, M. D. Sturge, and R. Bhat, J. Lumin. **35**, 235 (1986).

[54] *Semiconductor Statistics*, Dover Books on Physics and Chemistry, edited by J. S. Blakemore (Dover, New York, 1987).

[55] D. Paget, G. Lampel, B. Sapoval, and V. I. Safarov, Phys. Rev. B **15**, 5780 (1977).

[56] E. S. Artemova and I. A. Merkulov, Sov. Phys. Solid State **27**, 941 (1985).

[57] R. Giri, S. Cronenberger, M. M. Glazov, K. V. Kavokin, A. Lemaître, J. Bloch, M. Vladimirova, and D. Scalbert, Phys. Rev. Lett. **111**, 087603 (2013).

[58] H. Oohashi, H. Ando, and H. Kanbe, Phys. Rev. B **54**, 4702 (1996).

[59] I. I. Ryzhov, S. V. Poltavtsev, K. V. Kavokin, M. M. Glazov, G. G. Kozlov, M. Vladimirova, D. Scalbert *et al.*, Appl. Phys. Lett. **106**, 242405 (2015).

[60] A. Bechtold, D. Rauch, F. Li, T. Simmet, P.-L. Ardelt, A. Regler, K. Müller, N. A. Sinitsyn, and J. J. Finley, Nat. Phys., doi:10.1038/nphys3470 (2015).